Cell, Vol. 113, 383–394, May 2, 2003, Copyright ©2003 by Cell Press

Alternative Tertiary Structure of tRNA for Recognition by a Posttranscriptional Modification Enzyme

Ryuichiro Ishitani,[1,3] Osamu Nureki,[1,2,3,4] Nobukazu Nameki,[3] Norihiro Okada,[5] Susumu Nishimura,[6] and Shigeyuki Yokoyama,[1,2,3,*]

[1]Department of Biophysics and Biochemistry
Graduate School of Science
University of Tokyo
Hongo, Bunkyo-ku
Tokyo 113-0033
Japan

[2]RIKEN Harima Institute at SPring-8, 1-1-1 Kohto
Mikazuki-cho, Sayo
Hyogo 679-5148
Japan

[3]RIKEN Genomic Sciences Center, 1-7-22
Suehiro-cho, Tsurumi
Yokohama 230-0045
Japan

[4]PRESTO, JST

[5]Graduate School of Bioscience and Biotechnology
Tokyo Institute of Technology
4259 Nagatsuta-cho, Midori-ku
Yokohama 226-8501
Japan

[6]Banyu Tsukuba Research Institute (Merck)
3 Ookubo, Tsukuba 300-2611
Japan

Summary

Transfer RNA (tRNA) canonically has the clover-leaf secondary structure with the acceptor, D, anticodon, and T arms, which are folded into the L-shaped tertiary structure. To strengthen the L form, posttranscriptional modifications occur on nucleotides buried within the core, but the modification enzymes are paradoxically inaccessible to them in the L form. In this study, we determined the crystal structure of tRNA bound with archaeosine tRNA-guanine transglycosylase, which modifies G15 of the D arm in the core. The bound tRNA assumes an alternative conformation ("λ form") drastically different from the L form. All of the D-arm secondary base pairs and the canonical tertiary interactions are disrupted. Furthermore, a helical structure is reorganized, while the rest of the D arm is single stranded and protruded. Consequently, the enzyme precisely locates the exposed G15 in the active site, by counting the nucleotide number from G1 to G15 in the λ form.

Introduction

RNA molecules involved in translation and posttranscriptional RNA processing, such as tRNA, rRNA, and small nuclear RNA (snRNA), contain many modified nucleosides (Limbach et al., 1994; McCloskey and Crain, 1998), which are thought to be important for the RNA functions. Some of them are related to molecular recognition; the modified nucleosides found in the tRNA anticodon contribute to the high fidelity of codon recognition (Björk et al., 1999; Giegé et al., 1998; Marck and Grosjean, 2002; Yokoyama and Nishimura, 1995). Another important function of the modified nucleosides is in the structural formation and stabilization of the functional RNAs (Charette and Gray, 2000; Horie et al., 1985; Kawai et al., 1992; reviewed in Davis, 1998).

Many human diseases related to the structural formation of RNA emphasize the importance of the RNA modifications. In several mitochondrial diseases, mutations in tRNA genes reduce the modification level and the structural stability of the mitochondrial tRNAs, and thus may slow down the translation (Helm et al., 1999). On the other hand, there are several diseases related to deficiencies of RNA-modification enzymes, such as dyskeratosis congenita (DC). DC is an X-linked disorder characterized by premature aging and increased tumor susceptibility (Heiss et al., 1998). Patients with DC have a mutation in the gene encoding dyskerin/Cbf5p, a component of the box H/ACA small nucleolar ribonucleoprotein (snoRNP) complex, which is responsible for the pseudouridylation of snRNAs and rRNAs (Heiss et al., 1998; Lafontaine et al., 1998).

The importance of the modified nucleosides has also been investigated in bacterial systems. For example, a ribosome with an unmodified rRNA component has lower peptidyl-transfer activity as compared to that with the fully-modified rRNA (Green and Noller, 1999; Khaitovich et al., 1999). In *E. coli*, the deletion of the pseudouridine (Ψ) synthase for tRNA (TruB) or rRNA (RluD) resulted in impaired growth (Gutgsell et al., 2000; Ofengand, 2002). In addition, the RNA modification enzymes involved in the biosynthesis of these modified nucleosides may not only modify the nucleosides but also function as RNA chaperones, assisting in the correct folding of their substrate RNAs (Gutgsell et al., 2001; Ofengand, 2002).

The modified nucleosides involved in structural folding and stabilization usually form long-range, or tertiary, interactions. Typically, tRNA contains complex tertiary interactions (Kim et al., 1973). Most tertiary interactions of tRNA are centralized in its "core," which consists of the D arm and the variable loop (Figure 1A). The tRNA core contains many different modifications, such as s^4U8, m^1G9, m^2G10, Ψ13, m^1A22, m^2_2G26, m^7G46, and m^5C48. Moreover, the "L-shape" of the tRNA is established by the interaction between the D and T loops (Figure 1A). Several modifications (e.g., Gm18 and Ψ55) are involved in this tertiary interaction, which anchors the acceptor side to the anticodon side (Björk, 1995; Limbach et al., 1994; Marck and Grosjean, 2002; McCloskey and Crain, 1998; Sprinzl et al., 1998). The crystal structure of a complex of the tRNA Ψ55 synthase, TruB, and a T stem-loop RNA revealed that TruB gains access to U55 by a base-flipping mechanism (Hoang and Ferré-D'Amaré, 2001). By contrast, the modification sites in the tRNA core are buried more deeply and are involved in the complicated tertiary interactions described above.

*Correspondence: yokoyama@biochem.s.u-tokyo.ac.jp

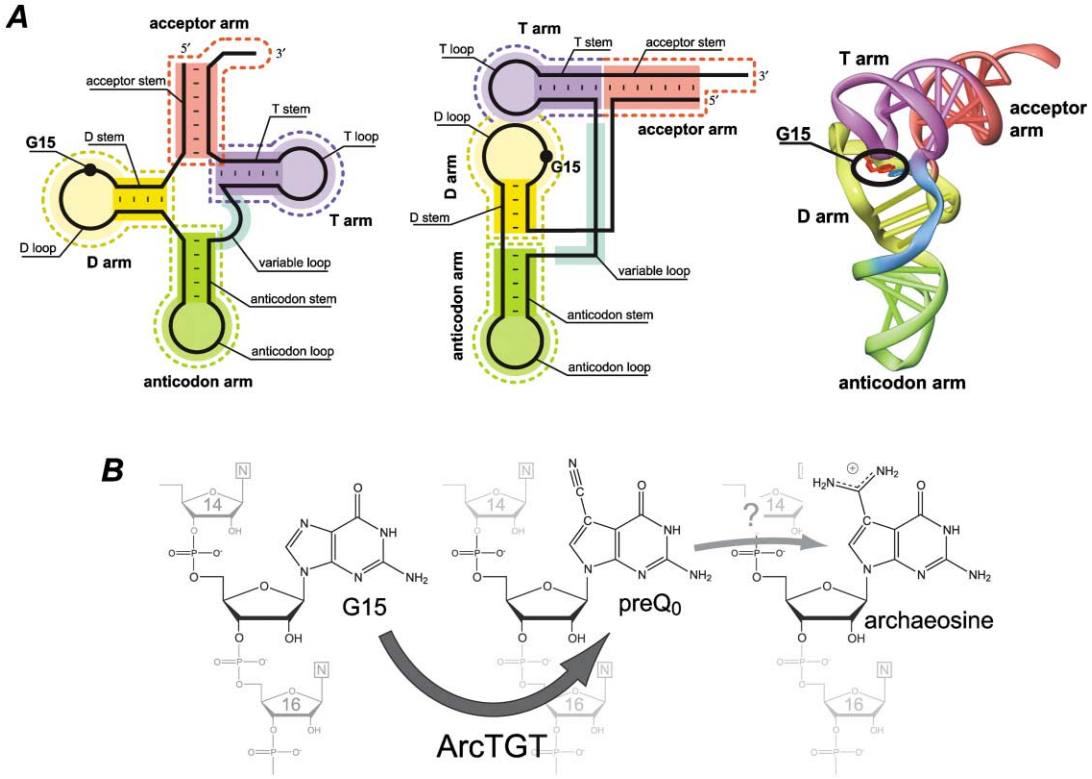

Figure 1. A tRNA Modification Enzyme, ArcTGT, Replaces the Base at Position 15 in the D Loop, which Is Deeply Buried in the Canonical L Form of tRNA

(A) The secondary and tertiary structures of tRNA in the canonical L form. The acceptor, D, anticodon, and T arms, and the variable loop are colored red, yellow, green, purple, and sky blue, respectively. The secondary structure is shown in the clover-leaf (left) and L-shape (center) diagrams. The RNA backbones are shown with thick lines, while the Watson-Crick base pairs are indicated with short thin lines. In the tertiary structure (right), the RNA backbone is shown as a tube model and the Watson-Crick base pairs are shown with sticks. The ArcTGT target site, G15, which is buried deeply in the tRNA tertiary structure, is circled.

(B) Biosynthetic pathway of archaeosine. The guanine moiety of G15 is replaced with $preQ_0$ by the transglycosylation catalyzed by ArcTGT. Afterwards, the $preQ_0$ at position 15 is further modified to archaeosine on the polynucleotide chain, by an unknown pathway (Watanabe et al., 1997). The biosynthetic pathway of $preQ_0$ is also unknown.

Hence, a more profound change in the tRNA conformation is necessary for the modification enzymes that target the tRNA core.

Archaeosine, 7-formamidino-7-deazaguanosine (Figure 1B), is a modified nucleoside widely found in archaea (Edmonds et al., 1991; Gregson et al., 1993; McCloskey et al., 2001). Archaeosine is present at position 15 in the tRNA D loop and is found within many tRNA isoacceptors (Gupta, 1984; Sprinzl et al., 1998). The nucleoside at position 15 interacts with position 48 in the variable loop and position 59 in the T loop. Thus, archaeosine is involved not only in the tRNA core formation, but also in the interaction between the D and T loops, which establishes the L-shape of the tRNA. Archaeosine therefore plays a crucial role as a wedge that strengthens the interactions among the variable, D, and T loops, which may tighten the tRNA structure.

Archaeosine tRNA-guanine transglycosylase (ArcTGT) is a key enzyme for the biosynthesis of archaeosine (Figure 1B). ArcTGT replaces the guanine base at position 15 of tRNAs with the free precursor, 7-cyano-7-deazaguanine ($preQ_0$), by cleaving and regenerating the *N*-glycosidic bond (Bai et al., 2000; Watanabe et al., 1997). To replace the base at the deeply buried position 15 (Figure 1A), ArcTGT must bind to a different tRNA structure, in which G15 may be exposed to the enzyme active site. Moreover, previous biochemical and structural studies of ArcTGT suggested that it precisely locates position 15 of the tRNA and specifically binds it to the catalytic center (Ishitani et al., 2002; Watanabe et al., 2000). However, ArcTGT has no sequence specificity to the other parts of the tRNA besides G15. Therefore, it is not understood how ArcTGT accurately locates position 15 of the tRNA without any primary structural information.

The C-terminal domains of the ArcTGTs contain a ubiquitously found RNA binding domain, the PUA (the pseudouridine synthase and archaeosine TGT) domain (Aravind and Koonin, 1999). The PUA domain of ArcTGT has high sequence homology to those of Cbf5p/dyskerin, which are responsible for the pseudouridylation of snRNAs and rRNAs, as noted above. Therefore, the PUA domains of Cbf5p/dyskerin and ArcTGT presumably share a common role as an RNA recognition domain. Moreover, the crystal structure of the ligand-free ArcTGT suggested that the large positively charged patch on the molecular surface of the C-terminal domains, including the PUA domain, of ArcTGT may recog-

Table 1. Data Collection and Refinement Statistics

Data collection statistics	
Wavelength (Å)	1.000
Resolution (Å)	50.0–3.3 (3.42–3.3)
Total reflections	334,265
Unique reflections	41,049
Completeness (%)	99.7 (99.8)
I/σ *(I)*	16.7 (2.31)
R_{sym} (%)	9.9 (48.7)
Refinement statistics	
Number of	
reflections used	41,391
protein atoms	9,286
RNA atoms	3,163
ions	6
water molecules	41
Rmsd of	
bond lengths (Å)	0.0119
bond angles (°)	1.57
improper angles (°)	1.49
R_{work} (%)	22.5
R_{free} (%)	28.8

nize the backbone phosphates of tRNA (Ishitani et al., 2002). Recently, it was pointed out that the C-terminal, RNA binding domain of the *E. coli* Ψ55 synthase, TruB, superimposes well on the PUA domain of ArcTGT, although there is no sequence homology between the two domains (Ferré-D'Amaré, 2003). However, the actual roles of the eukaryotic and archaeal PUA domains remain elusive.

In the present study, we determined the crystal structure of the *Pyrococcus horikoshii* ArcTGT complexed with $tRNA^{Val}$ at 3.3 Å resolution. This is, to our knowledge, the first structure determination of a tRNA modification enzyme bound to a full-length tRNA. We revealed that the tRNA modification enzyme binds a surprisingly different tRNA conformation ("λ form"), in which the canonical core is completely disrupted and the melted D arm is protruded. Moreover, the PUA domain was found to be crucial for the precise location of the tRNA molecule on the enzyme.

Results and Discussion

Overall Structure

The crystal structure of the ArcTGT·$tRNA^{Val}$ complex was solved by molecular replacement, using the tRNA-free ArcTGT structure (Ishitani et al., 2002) as a search model (Table 1; Supplemental Figure S1 available at http://www.cell.com/cgi/content/full/113/3/383/DC1). The asymmetric unit of the ArcTGT·$tRNA^{Val}$ crystal contains one ArcTGT dimer (subunits A and B; Figure 2A) and two $tRNA^{Val}$ molecules (tRNAs I and II; Figure 2A). As expected from the tRNA-free ArcTGT structure (Ishitani et al., 2002), each tRNA is bound with both of the two subunits of ArcTGT (Figure 2A). The backbone structures of the tRNA-bound and tRNA-free ArcTGTs are mostly the same, but several residues near the catalytic site exhibit different conformations. The dimerization manner of ArcTGT in the tRNA-bound form is also the same as that in the free form. There is no considerable structural difference either between the A and B subunits of the protein or between the two tRNA molecules, I and II, bound to the protein. As the tRNA-I molecule bears lower *B* factors than the tRNA-II molecule, we hereafter describe the complex structure focusing on the tRNA-I molecule, unless otherwise stated.

The crystal structure of the ArcTGT·$tRNA^{Val}$ complex features the following points. First, the structure of the tRNA in the complex (here named the "λ form") is strikingly different from the canonical L-shaped tRNA structure (Figures 3A and 3B). In the λ form, the nucleotide residues U8 through U22 of the D arm protrude, while the rest of the D stem and the variable loop form a new helical structure (Figures 3A and 3B). We propose the possibility that the λ form is also assumed by tRNAs in other systems. Second, the C-terminal domains of the A subunit recognize the tRNA acceptor stem (Figures 2A and 5C). Third, the catalytic domain of the B subunit binds the protruded part (U8–U17) of the D arm (Figures 2C). In this order, the details of the complex structure are described below.

Novel Tertiary Structure of tRNA

In the λ form, the nucleotide residues U8–U22 of the D arm protrude from the body of the tRNA (Figure 3A). This drastic change results from the complete reorganization of the "core" of the L-shaped structure. In the canonical form (designated hereafter as the "L form"), the D stem is formed by the base pairing of G10, U11, C12, and U13 with C25, A24, G23, and U22, respectively (Figures 1A and 3B). Furthermore, the D arm and the variable loop are tightly connected by the tertiary base pairs and triples (long-range two-base and three-base interactions, respectively), G10:C25:G45, G9:C12:G23, U13:U22:G46, U8:A14, G15:C48 (Figure 1A and 4B), which form the "core" of the canonical L shape. In the λ-form tRNA, all of the base-base interactions for the formation of the D stem and the canonical core are completely disrupted. Thus, the entire region from U8 to U22 is not base paired in the λ form (Figures 2D and 3A).

On the other hand, G23-A24-C25 forms Watson-Crick base pairs with G46-U47-C48 in the variable loop (Figures 2D and 3A), and the top base pair (G23:C48) stacks with the A59 nucleotide residue in the T loop (Figure 4A). This long-range interaction is reminiscent of the A59 and C48:G15 interactions in the canonical core (Figure 4B). Next to this "stem," there is the "internal loop" consisting of G26, A44, and G45 (Figure 4A). This reorganization in the D-arm and variable-loop regions forms a new base-stacked double-helical structure, which is designated hereafter as the "DV helix." Thus, in the λ-form tRNA, the "DV helix" has replaced the canonical core.

The secondary structures of all tRNAs from *P. horikoshii* and *E. coli*, except for those with a long variable arm (type-II tRNA), can be reorganized to form a similar "DV helix" (Supplemental Figure S2 available at http://www.cell.com/cgi/content/full/113/3/383/DC1). These DV helices are characterized by the presence of non-Watson-Crick base pairs, and should be much less rigid than the canonical core. Actually, we prepared an unnatural tRNA variant with a DV helix rich in purine-purine mismatches, and found that its transglycosylation activity was as high as 24% of that of the normal

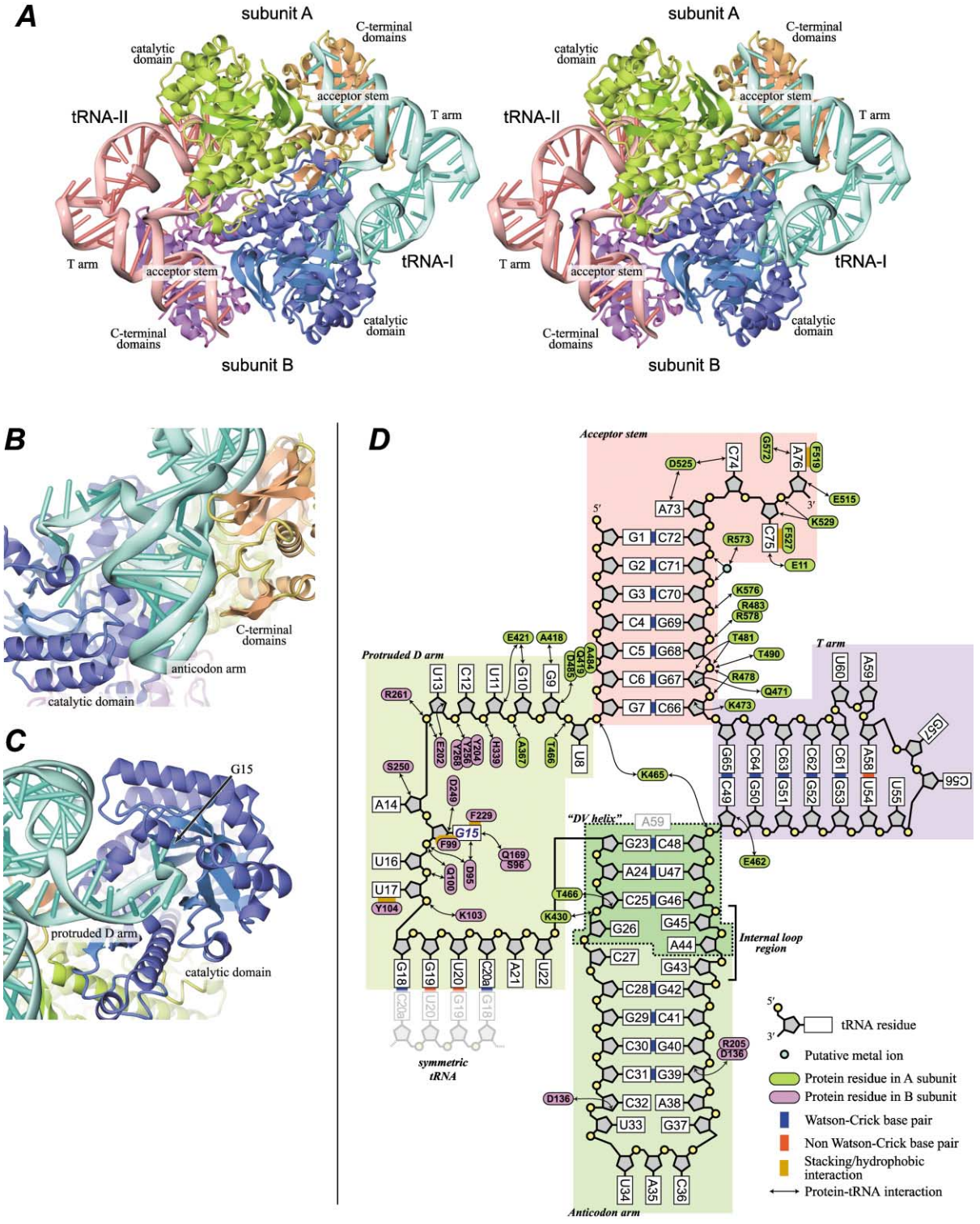

Figure 2. Overall Structure of the *P. horikoshii* ArcTGT·tRNA^{Val} Complex

(A) Stereo view of the ArcTGT·tRNA^{Val} complex. ArcTGT and tRNA are shown as ribbon models. The catalytic domain and the C-terminal domains of the ArcTGT subunit A are colored green and brown, while those of subunit B are colored deep blue and purple, respectively. tRNA-I and -II are colored sky blue and pink, respectively.

(B and C) Close-ups of the ArcTGT-tRNA interaction interfaces. (B) The anticodon arm and the DV helix are accommodated into the cleft formed between the catalytic and C-terminal domains. (C) U8 to U17 of the protruded D arm are recognized by the C-terminal domains of subunit A and the catalytic domain of subunit B, and G15 is accommodated into the catalytic pocket. The coloring schemes of (B) and (C) are the same as in (A).

(D) Schematic diagram of the ArcTGT-tRNA interactions.

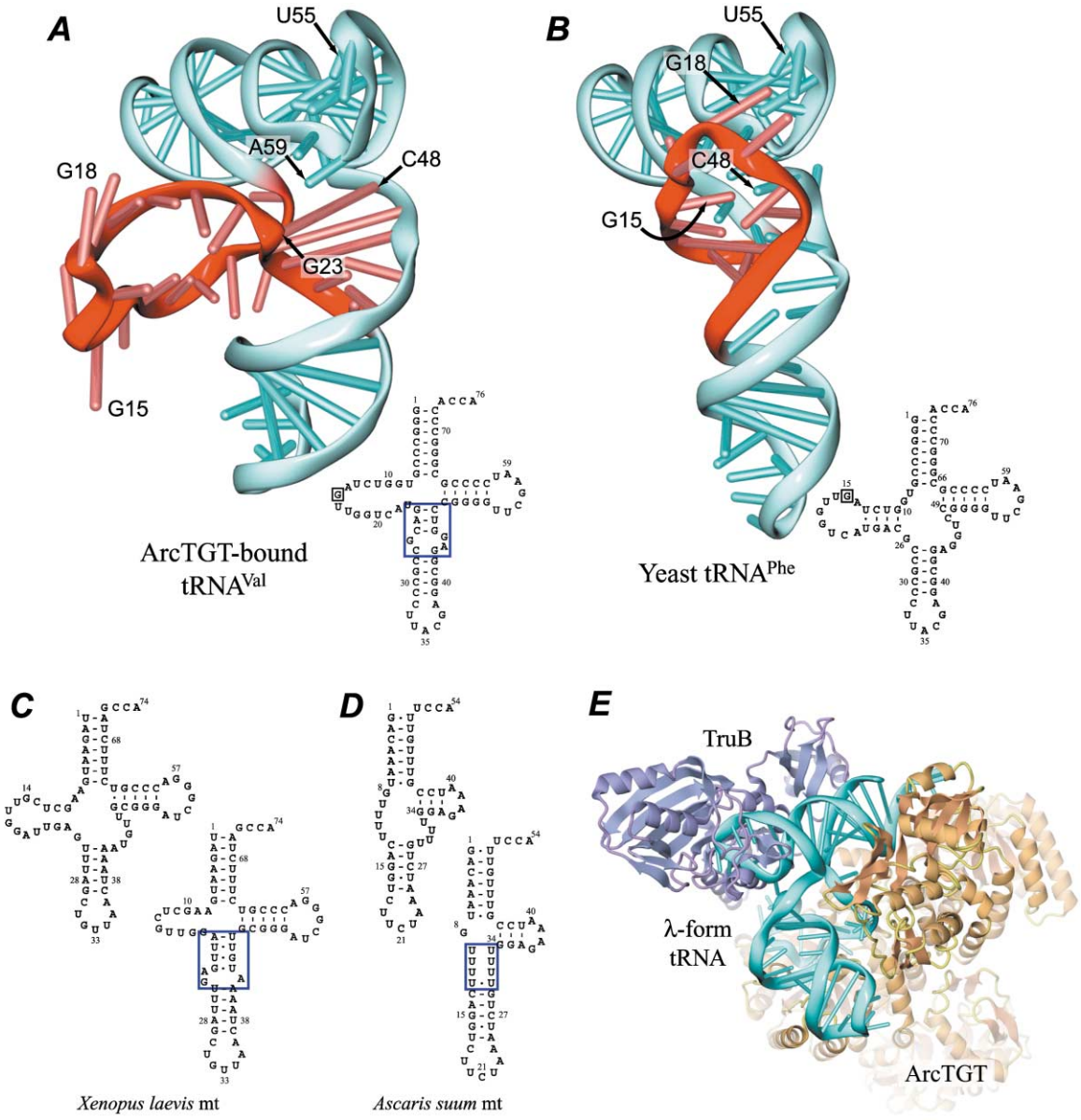

Figure 3. The λ Form of tRNA

(A) Ribbon model and secondary structure of the ArcTGT-bound $tRNA^{Val}$ in the λ form. The nucleotide residues in the protruded D arm and DV helix are colored red.

(B) Ribbon model and secondary structure of the yeast $tRNA^{Phe}$ (Shi and Moore, 2000) for comparison. The corresponding nucleotide residues are colored the same as in (A).

(C and D) Schematic drawings of the secondary structures of *X. laevis* mt $tRNA^{Asn}_{GUU}$ (C) (Roe et al., 1985) and *A. suum* mt $tRNA^{Ser}_{UCU}$ (D) (Okimoto et al., 1992). For each tRNA, the canonical- and λ-form secondary structures are shown in the upper and lower rows, respectively. In the λ-form structures, the DV helices are indicated by blue rectangles. The short lines between bases denote canonical pairs, while the dots denote non-canonical pairs.

(E) Docking model of the ArcTGT·tRNA complex and the TruB Ψ55 synthase. ArcTGT, TruB, and λ-form tRNA are shown as ribbon models, and are colored brown, purple, and sky blue, respectively. TruB was docked so that the T stem-loop RNA in the TruB·RNA complex structure (Hoang and Ferré-D'Amaré, 2001; PDB entry 1K8W) is superimposed onto the T arm of the ArcTGT-bound tRNA.

tRNA (data not shown). Therefore, the continuous Watson-Crick base pairs in the DV helix are not important for the tRNA to assume the λ form. The DV helix and the anticodon stem are connected to form a double-helical structure, with the axis kinked by about 30 degrees at the internal loop (Figures 3A and 4A). The top base pair of the anticodon stem (C27:G43) is distorted and is therefore non-hydrogen-bonded, which may be ascribed to the internal loop (Figure 4A). The DV helix and the anticodon stem are entirely docked in the cleft between the catalytic domain and the C-terminal domains (Figure 2B). Specifically, the DV helix seems to be stabilized by the tRNA-protein interactions described below.

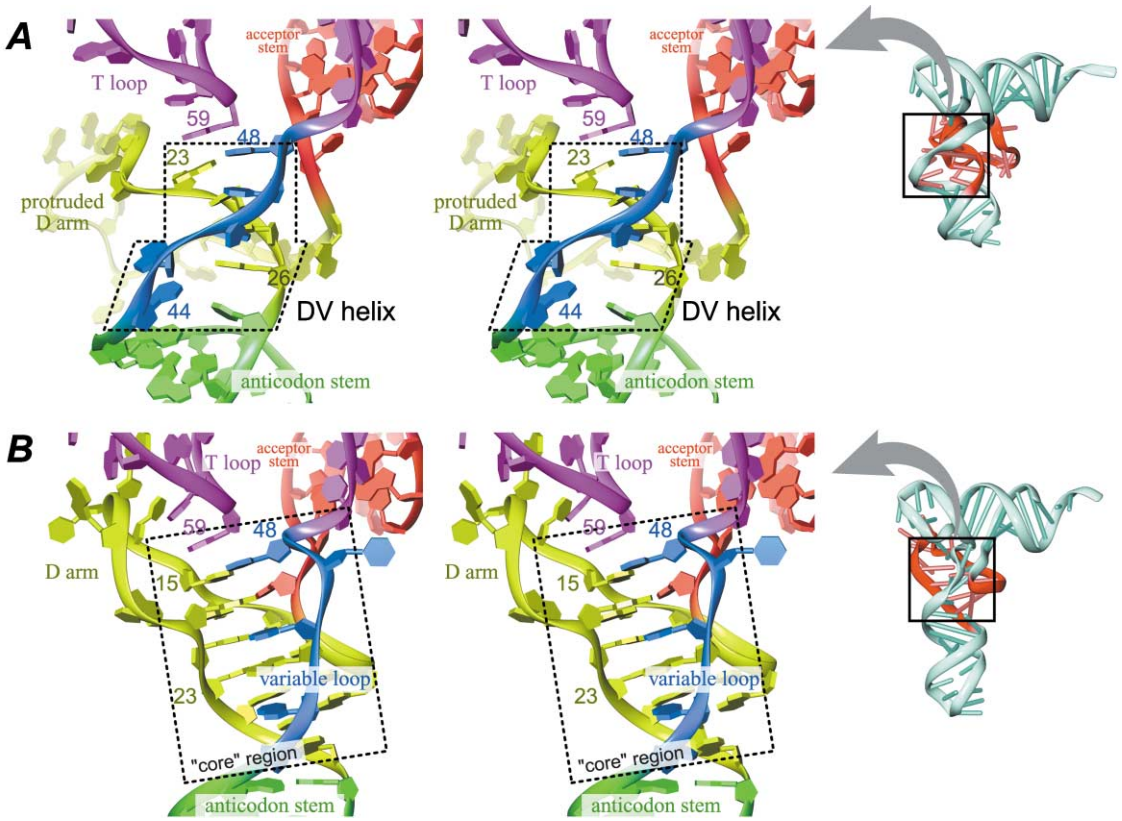

Figure 4. Structural Comparison of the DV Helix in the λ-Form tRNA and the Canonical Core in the L-Form tRNA

(A) The DV helix and its surrounding structures in the λ-form tRNA (stereo view). The nucleotide backbones are represented by ribbon models. The acceptor-, T-, D-, anticodon-arms, and variable-loop regions are colored red, purple, yellow, green, and blue, respectively. The DV helix is indicated with dashed lines.

(B) Stereo view of the core structure of the canonical L-form tRNA (yeast $tRNA^{Phe}$; Shi and Moore, 2000). The coloring schemes are the same as in (A). The canonical core structure is indicated with a dashed rectangle.

In contrast, the conformation of the T loop is roughly the same as that of the canonical tRNA, despite the absence of the canonical tertiary interactions with the invariant G18-G19 in the D loop. The structures of the T and acceptor arms in the λ form are almost the same as those of the L form (Figures 3A and 3B).

Mitochondrial tRNA in the λ Form

Intriguingly, tRNA secondary structures similar to that of the λ form are found in mitochondria (mt) (Okimoto and Wolstenholme, 1990; Wolstenholme et al., 1987). For example, *Xenopus laevis* mt $tRNA^{Asn}_{GUU}$ (Roe et al., 1985) cannot form the canonical D-stem base pairs, although it has a D arm with nearly the same length as that of the normal tRNA (Figure 3C). The mt $tRNA^{Asn}$ can form the DV helix, and the secondary structure is like that of the λ form (Figure 3C). Furthermore, *Ascaris suum* mt $tRNA^{Ser}_{UCU}$ (Okimoto et al., 1992) lacks most of the D arm (Figure 3D). The structural analysis of *A. suum* mt $tRNA^{Ser}$ in solution suggested that its variable loop and shortened D arm form a flexible stem ("connector region") that stacks on the anticodon stem (Figure 3D; Ohtsuki et al., 2002). The bottom uridines of the connector region are base paired, while other uridines form a base-stacked stem-like structure (Figure 3D). The connector region of the mt $tRNA^{Ser}$ also resembles the DV helix of the λ-form tRNA (Figure 3D).

Roles of the DV Helix

The canonical L form has the tight core structure made by the D-arm and the variable loop. In contrast, the same tRNA regions assume the un-base-paired loop and the soft DV helix conformations in the λ form. The former is for the access of G15 to ArcTGT, and the un-base-paired region is protected by the protein (see below). As for the DV helix, one possible role is to protect the regions from degradation or aggregation, as the same regions are protected by the canonical core formation in the L form. The DV helix may also prevent the propagation of the base pair disruption to the anticodon and T stems of the tRNA. On the other hand, after the modification, the tRNA should refold to the canonical L form, because the λ-form tRNA may not function in aminoacylation and translation, and may be prone to degradation or aggregation. Therefore, the non-rigid nature of the DV helix, described above, is probably suitable for the efficient refolding to the canonical L form.

Possible Involvement of the λ-Form tRNA in Other Modification Processes

The present study of the ArcTGT·tRNA complex revealed that the modification enzyme targeting the tRNA core binds the λ-form tRNA. In addition to archaeosine, which is unique to archaea, several modifications, such as s^4U8, m^1G9, m^2G10, Ψ13, and m^1A22, within the tRNA

core are found in one or more of the three phylogenic domains (Sprinzl et al., 1998). Therefore, it is possible that the modification enzymes for those modified nucleosides also recognize the protruded D arm of the λ-form tRNA.

Similarly, the T loop in the λ-form tRNA is accessible to enzymes, because the canonical interactions between the D and T loops (G18:U55 and G19:C56) are disrupted (Figure 3A). Actually, the tRNA Ψ55 synthase, TruB, can access U55 more easily in the λ form than in the L form, according to the crystal structure of the T stem-loop RNA·TruB complex (Hoang and Ferré-D'Amaré, 2001). Moreover, TruB recognizes the acceptor stem from the opposite side to the ArcTGT. Thus, both enzymes can bind with the λ-form tRNA simultaneously (Figure 3E). The conformational transition between the L and λ forms might be a rate-limiting step for each modification enzyme. However, once the tRNA conformation has changed to the λ form, the modification enzymes may successively bind it and modify their target sites one after another, as in this docking model (Figure 3E). Therefore, it is feasible that the tRNA modification enzymes, as well as the processing enzymes, are localized in the cell and form a weak complex, which may be something like a factory for tRNA maturation ("modificosome").

ArcTGT C-Terminal Domains Recognize the tRNA Acceptor Stem

In contrast to the DV helix and anticodon arm, the acceptor stem is tightly recognized by the C-terminal domains of ArcTGT (Figure 2D). The basic residues, Arg573, Lys576, and Arg578, on the β sheet of domain C3 electrostatically interact with the backbone phosphates of G69 to C72 (Figures 2D and 5A). The pattern of the positively-charged patch on the surface of domain C3 (Figure 5B) is complementary to the negatively-charged phosphates of the 3′ strand of the acceptor stem. Domain C3 is the PUA domain (Aravind and Koonin, 1999), which is widely found throughout the RNA modification enzymes from eukaryotes and archaea. Specifically, the basic residues involved in the RNA recognition described above (Lys576 and Arg578) are conserved among the PUA domains of Cbf5p (Figure 5A and Supplemental Figure S3 available at URL above), which is a catalytic component of the box H/ACA snoRNP and is responsible for the Ψ formation in rRNAs and snRNAs (Lafontaine et al., 1998; Watkins et al., 1998). Ferré-D'Amaré (2003) found that the structure of an RNA binding domain of the *E. coli* TruB (Hoang and Ferré-D'Amaré, 2001) superimposes well on that of the PUA domain of ArcTGT (Ishitani et al., 2002), although no sequence homology between the two enzymes is detectable. The present complex structure revealed that the RNA binding modes of the TruB and ArcTGT domains are different (Figure 5D). Nevertheless, it is worth pointing out that Arg307 in TruB may have a similar role to that of Arg578 in ArcTGT.

The main chain of the residues (Lys522, Gly523, and Lys524) in domain C3 recognizes the 5′ end of the acceptor stem (Figures 5B and 5C). Thus, the molecular surface of domain C3 snugly fits on the terminus of the acceptor stem (Figures 5B and 5C). If there were one more base pair on the top, it would cause a serious steric hindrance with domain C3. On the other hand, the CCA-terminal residues of the tRNA are stacked with the Phe residues (C75 and Phe527, and A76 and Phe519, respectively) in domain C3 (Figure 5A), which are highly conserved in ArcTGT (Supplemental Figure S3). A previous biochemical analysis suggested that the CCA-terminal residues are not required for the recognition by ArcTGT (Watanabe et al., 2000), which is feasible since premature tRNAs often lack these residues (Aebi et al., 1990). Therefore, the interactions may simply anchor the CCA-terminal residues to the side of domain C3 for protection from degradation.

The polar residues, Arg483, Arg478, Gln471, Thr481, and Thr490, on the β sheet in domain C2 interact with the backbone phosphates of C66 to G69 (Figure 2D). The surface of domain C2 also forms a positively charged patch, which snugly fits the phosphates of the 3′ strand of the acceptor stem and is continuous with that of domain C3 (Figure 5B). Therefore, domains C2 and C3 collaborate to locate all of the acceptor-stem base pairs (1:72 to 7:66) accurately.

A β Hairpin in Domain C2 Stabilizes the λ Form tRNA

The tip of the β18β19 hairpin (Lys465 to Thr466), which protrudes from the flat RNA binding surface formed by domains C2 and C3, is thrust into the underarm of the L-shaped portion of the λ-form tRNA (Figure 5B). The main chain carbonyl oxygen of Thr466 hydrogen bonds with the 2′-hydroxyl group of C25 (Figure 2D). The side chain of Lys465 is flanked by the phosphates of U8 and C49, with which it electrostatically interacts (Figure 2D). In the λ-form tRNA, C25 and C48 are involved in the DV helix. U8 and its subsequent nucleotides (G9 to U17) are un-base-paired and bound to ArcTGT. On the other hand, if we dock the canonical L-form tRNA to ArcTGT so that the acceptor and T stems are superimposed on those of the λ-form tRNA, then the β18β19 hairpin causes a steric clash against U8, C25, and C48. Therefore, the β18β19 hairpin may be important for the λ-form tRNA recognition. We constructed a deletion mutant lacking residues 463 to 466 (Δ(463–466)), and assayed the transglycosylation activity. We could not detect any activity with this deletion mutant (data not shown), which also suggests that the β18β19 hairpin plays a crucial role in the recognition of the λ-form tRNA.

ArcTGT Counts the Nucleotide Number between Positions 1 and 15

As already described above, the entire stem-loop structure of the D arm is completely disrupted, and nucleotide residues U8 to U22 are stretched out from the tRNA body. The first part of the stretched residues (U8 to U13) is bound to the cleft, formed by the two subunits of ArcTGT (Figure 6A). The phosphate backbone of these nucleotide residues is recognized by the hydrophilic residues of ArcTGT (Figures 2D and 6A). On the other hand, the base moieties of these nucleotide residues are stacked with each other and are not recognized by ArcTGT, except for G9 and G10 (Figures 2D and 6A). The 2-amino groups of G9 and G10 hydrogen bond with the backbone carbonyl group of Ala418 and the side chain of Glu421, respectively. The A14, G15, and U16 nucleotides are bound to the catalytic domain of ArcTGT

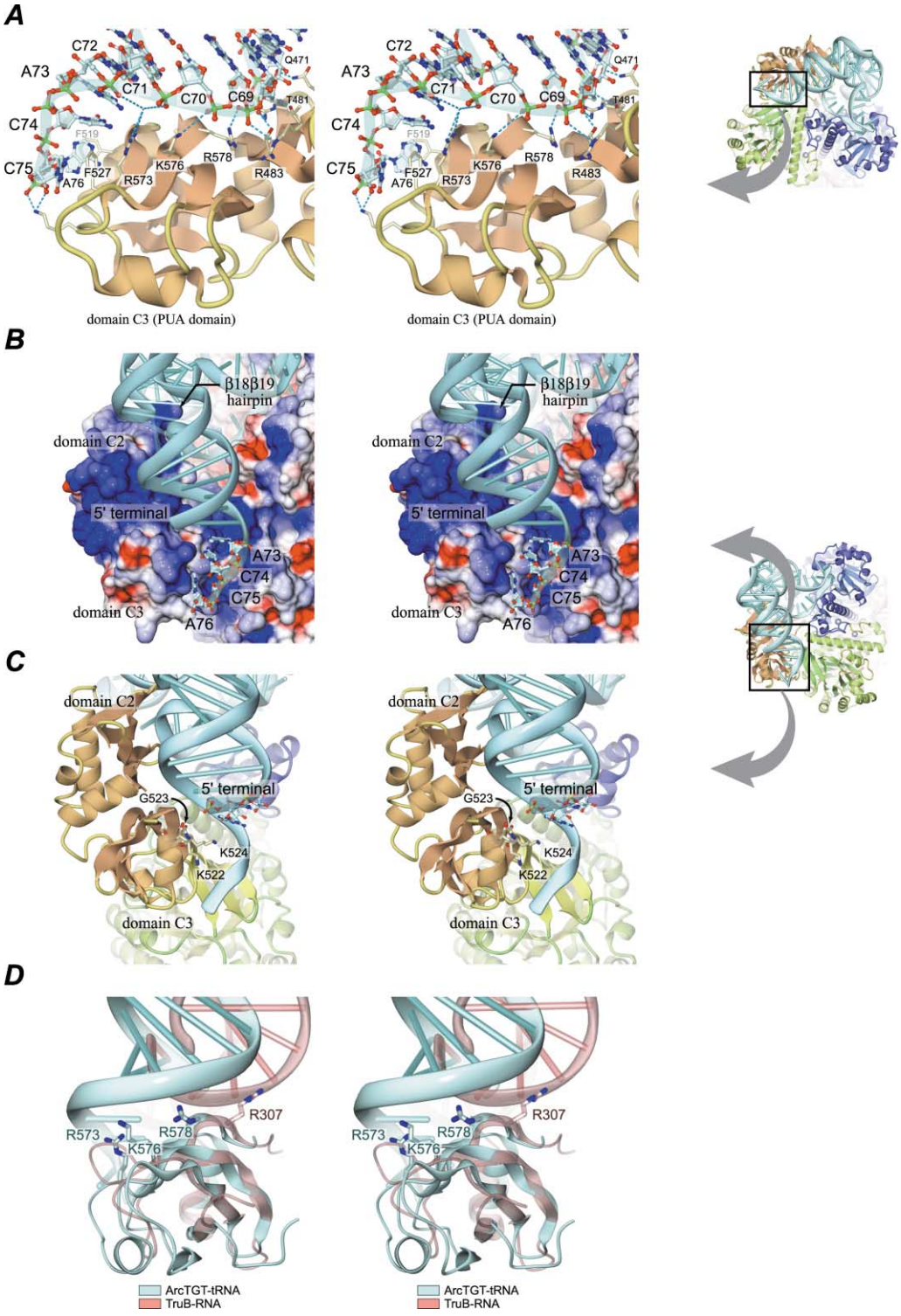

Figure 5. The tRNA Acceptor Stem Recognition by the C-Terminal Domains of ArcTGT

(A) Domain C3 (the PUA domain) recognizes the tRNA acceptor stem and the CCA-terminus (stereo view). The protein is shown as a ribbon model. The tRNA is shown as a ball-and-stick model. The interactions between the protein and the tRNA are indicated by dashed lines.

(B and C) The shape and the surface charge of the C-terminal domains snugly fit with those of the tRNA acceptor stem (stereo views). (B) The protein is shown as a solvent-excluded surface, and the tRNA is shown as a ribbon model. The protein surface is colored by its electrostatic potential, from red (−10 *kT*/*e*) to blue (10 *kT*/*e*). The solvent-accessible surface was generated with the program MSMS (Sanner et al., 1995), and the electrostatic potential was calculated with the program Grasp (Nicholls et al., 1991). (C) Both the protein and tRNA are shown as ribbon models. The tRNA 5′-residue and K522, G523, and K524 of the protein are shown as stick models.

(D) Superposition of the ArcTGT PUA domain (light blue) and the TruB C-terminal domain (pink) with their RNA substrates (stereo view). The RNA-interacting basic amino acid residues are labeled.

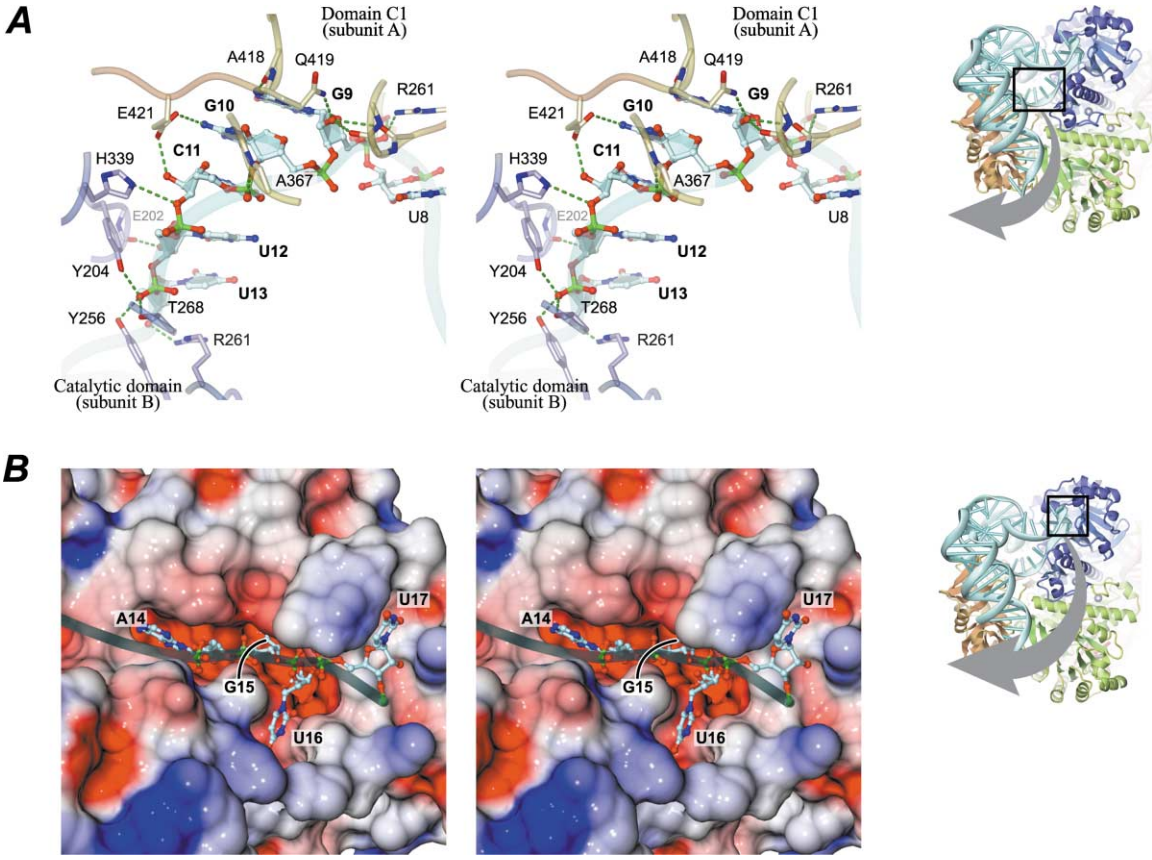

Figure 6. Protruded D Arm Recognition by the C-Terminal and Catalytic Domains of ArcTGT

(A) The protruded nucleotide residues of the D arm (G9 to U13) are bound to the cleft formed by the two subunits of ArcTGT (stereo view). Subunits A and B of ArcTGT are shown as yellow and blue ribbon models, respectively. The tRNA backbone is shown as a transparent tube. The protein and tRNA residues involved in the protein-tRNA interactions are shown as stick models. The protein-tRNA interactions are indicated by dashed lines.

(B) Surface model of the catalytic domain of tRNA-bound ArcTGT (stereo view). The surface model is colored as in Figure 5B. The nucleotide residues A14, G15, U16, and U17 are shown as ball-and-stick models. The tRNA backbone is shown as a transparent tube.

(Figures 2D and 6B). The A14 and U16 nucleotide residues are bound to the pockets formed at the edge of the $(\alpha/\beta)_8$ barrel, whereas the G15 nucleotide residue is buried deeply within its center. Both the A14 and U16 pockets are mainly composed of hydrophobic residues and are large enough to accommodate purine bases, which suggests that these pockets do not provide base-specific recognition. On the other hand, the base moiety of G15, which is the target site for the base-exchange reaction, is specifically recognized in a similar manner to that seen in the ArcTGT·guanine complex structure (Ishitani et al., 2002).

Previous biochemical results suggested that ArcTGT specifically recognizes G15 without any primary structural information of the tRNA (Watanabe et al., 2000). Mutants at positions 8 to 14 retained the same guanine-exchanging activity as the intact tRNA, whereas mutants at position 15 abolished the activity. Moreover, insertion or deletion mutants at positions 8 to 14 considerably reduced the activity. This tRNA recognition mechanism can be clearly explained by the present complex structure. First, the tight recognition of the tRNA acceptor stem by domains C2 and C3, including the β18β19 hairpin, enables ArcTGT to count the number of the acceptor stem pairs (from 1:72 to 7:66; Figure 2D). Next, ArcTGT precisely counts bases within the un-base-paired D arm from positions 8 to 13 by recognizing their backbone phosphates and sugars one by one (Figure 2D). Finally, the nucleotide residues at positions 14, 15, and 16 are correctly bound to the pockets on the catalytic domain (Figure 2D), as described above.

Concluding Remarks

The present crystal structure revealed that a tRNA modification enzyme modifies its buried target site by recognizing a tRNA with a profound conformational change, in which the tRNA is not denatured but in an alternative conformation, the λ form. The λ form of tRNA provides a scaffold for modification enzyme binding. In addition, the λ-form formation may protect the unrecognized parts of the tRNA from enzymatic and/or chemical degradation. Hence, the λ-form formation may be indispensable for the modification.

This mechanism of structurally-reorganized RNA recognition may also be found in other RNA modification systems. For example, eukaryotic snRNAs and rRNAs are modified in the nucleolus by base pairing with sno-

RNAs, which have complementary sequences to the modification target sites and serve as guides for the modification (reviewed in Kiss, 2001, 2002). The base pairing between rRNA/snRNA and snoRNA may be a remarkable example of the structural reorganization taking place in RNA modification.

In the RNA modification by the snoRNP complex noted above, its catalytic protein component modifies the RNA target site by recognizing the rRNA/snRNA-snoRNA duplex and the conserved sequence in the snoRNA. The distance from the conserved sequence to the target site is important for the target-site determination (Kiss, 2001, 2002). Among the snoRNP components, Cbf5p, which is responsible for the Ψ formation in rRNAs and snRNAs, contains the PUA domain. Therefore, we speculate that the PUA domains of ArcTGT and Cbf5p share a common role in the "position-specific" RNA recognition. The position-specific tRNA recognition revealed in the present study provides a structural basis for understanding such RNA recognition in the nucleolus.

Experimental Procedures

Crystallization and Data Collection

Overproduction and purification of the *P. horikoshii* ArcTGT were performed using a method similar to that described elsewhere (Ishitani et al., 2001). The *P. horikoshii* $tRNA^{Val}$ isoacceptor with the UAC anticodon was transcribed in vitro with T7 RNA polymerase. Crystals were grown at 20°C by the hanging-drop vapor diffusion method. The protein/tRNA solution for crystallization was prepared at a final protein concentration of 6–8 mg ml^{-1}, for a molar ratio of ArcTGT and tRNA of 1:1. A 1 μl aliquot of the protein/tRNA solution was mixed with 1 μl of a crystallization solution, composed of 100 mM citrate buffer (pH 5.6) containing 1.0 M ammonium dihydrogen phosphate and 0.3% xylitol. The drop solution was slowly equilibrated against a reservoir solution, composed of 100 mM citrate buffer (pH 5.6) containing 1.0 M ammonium dihydrogen phosphate and 400 mM sodium chloride. Crystals grew to dimensions of 100 × 100 × 100 μm in the course of 2 months.

For data collection under cryogenic conditions, the crystals were briefly transferred to a solution of 100 mM citrate buffer (pH 5.6) containing 1.2 M ammonium dihydrogen phosphate and 25% (v/v) glycerol, and were flash-cooled by a cryo-stream of helium gas at 100 K. The dataset of the crystal was collected at 30 K at station BL41XU of SPring-8 (Harima, Japan). The helium cryo-stream at 30 K considerably reduced the X-ray damage, as compared to the nitrogen cryo-stream at 100 K. The resulting dataset was processed with the program suite HKL2000 (Otwinowski and Minor, 1997). The crystal belongs to the space group *R*32, with unit cell dimensions of a = b = 230.8 Å, c =269.3 Å, α =β =90°, and γ = 120°.

Structure Determination and Refinement

Using the free-form ArcTGT structure (Ishitani et al., 2002; PDB entry 1IQ8) as a search model, molecular replacement was performed by the program MOLREP (Vagin and Teplyakov, 1997). The solution was further refined with the program CNS (Brünger et al., 1998), by rigid-body refinement procedures. In the resultant $2m|F_o| - D|F_c|$ and $m|F_o| - D|F_c|$ maps, we clearly found the tRNA electron densities. The models of the tRNAs were built using the program O (Jones et al., 1991), and were refined with CNS by energy minimization and simulated annealing procedures. Non-crystallographic symmetry restraints (weight = 300 kcal mol^{-1} $Å^{-2}$) were only applied on the main-chain coordinates of each protein monomer. Finally, the ArcTGT·$tRNA^{Val}$ model structure was refined with an *R*-factor of 22.5% (R_{free} = 28.8%) up to 3.3 Å resolution. The Ramachandran plot analysis with the program PROCHECK (Laskowski et al., 1993) showed that 99.2% of the protein residues are in the most favored and additionally allowed regions. Molecular graphics pictures in Figures 1–6 were prepared by using the programs Que (http://www.biochem.s.u-tokyo.ac.jp/~ishitani/que/) and Dino (http://www.dino3d.org/).

Mutational Analyses

The ArcTGT mutation, Δ(463–466), was introduced as described (Ishitani et al., 2002). The mutants were overproduced and purified in the same way as the wild-type ArcTGT. The correct folding of the Δ(463–466) mutant was confirmed by the dynamic light scattering analysis (data not shown). The tRNA variant with the mismatched DV helix (from 45-GGUC-48 to 45-AAG-48) was constructed and transcribed in vitro by T7 RNA polymerase, as described (Watanabe et al., 2000). The guanine-exchange activity was assayed as described (Watanabe et al., 2000). The 60 μl reaction mixture contained 50 mM Tris-HCl buffer (pH 7.5) containing 5 mM $MgCl_2$, 400 mM NaCl, and 10 μM [8-^{14}C]guanine hydrochloride. The concentrations of ArcTGT and tRNA were fixed to 80 μM and 300 nM, respectively. The initial velocity (V_0) of the guanine-exchange activity was measured at 45°C. The relative activity of each mutant was defined as the ratio of the initial velocity to that of the normal $tRNA^{Val}$ catalyzed by the wild-type enzyme.

Acknowledgments

We acknowledge the contributions of Drs. M. Kawamoto, H. Sakai, and N. Kamiya for the synchrotron data collection at SPring-8. We are grateful to Dr. M. Watanabe and Mr. T. Kijimoto, of the Graduate School of Bioscience and Biotechnology, Tokyo Institute of Technology, Japan, for providing the over-expression vector of the *P. horikoshii* ArcTGT. We thank Drs. Y. Watanabe, T. Hirota, and M. Hara-Yokoyama for their helpful comments on the manuscript. This work was supported in part by Grants-in-Aid for Scientific Research from the Ministry of Education, Culture, Sports, Science, and Technology (MEXT) of Japan, and by the National Project on Protein Structural and Functional Analyses of MEXT.

Received: December 31, 2002
Revised: February 28, 2003
Accepted: March 25, 2003
Published: May 1, 2003

References

Aebi, M., Kirchner, G., Chen, J.Y., Vijayraghavan, U., Jacobson, A., Martin, N.C., and Abelson, J. (1990). Isolation of a temperature-sensitive mutant with an altered tRNA nucleotidyltransferase and cloning of the gene encoding tRNA nucleotidyltransferase in the yeast Saccharomyces cerevisiae. J. Biol. Chem. *265*, 16216–16220.

Aravind, L., and Koonin, E.V. (1999). Novel predicted RNA-binding domains associated with the translation machinery. J. Mol. Evol. *48*, 291–302.

Bai, Y., Fox, D.T., Lacy, J.A., Van Lanen, S.G., and Iwata-Reuyl, D. (2000). Hypermodification of tRNA in Thermophilic archaea. Cloning, overexpression, and characterization of tRNA-guanine transglycosylase from *Methanococcus jannaschii*. J. Biol. Chem. *275*, 28731–28738.

Björk, G.R. (1995). Biosynthesis and function of modified nucleosides. In tRNA: Structure, Biosynthesis, and Function, D. Söll, and U. RajBhandary, eds., pp. 165–205.

Björk, G.R., Durand, J.M., Hagervall, T.G., Leipuviene, R., Lundgren, H.K., Nilsson, K., Chen, P., Qian, Q., and Urbonavicius, J. (1999). Transfer RNA modification: influence on translational frameshifting and metabolism. FEBS Lett. *452*, 47–51.

Brünger, A.T., Adams, P.D., Clore, G.M., DeLano, W.L., Gros, P., Grosse-Kunstleve, R.W., Jiang, J.S., Kuszewski, J., Nilges, M., Pannu, N.S., et al. (1998). Crystallography & NMR system: A new software suite for macromolecular structure determination. Acta Crystallogr. *D54*, 905–921.

Charette, M., and Gray, M.W. (2000). Pseudouridine in RNA: what, where, how, and why. IUBMB Life *49*, 341–351.

Davis, D.R. (1998). Biophysical and conformational properties of modified nucleosides in RNA (nuclear magnetic resonance studies).

In Modification and Editing of RNA, H. Grosjean, and R. Benne, eds. (ASM Press), pp. 85–102.

Edmonds, C.G., Crain, P.F., Gupta, R., Hashizume, T., Hocart, C.H., Kowalak, J.A., Pomerantz, S.C., Stetter, K.O., and McCloskey, J.A. (1991). Posttranscriptional modification of tRNA in thermophilic archaea (Archaebacteria). J. Bacteriol. *173*, 3138–3148.

Ferré-D'Amaré, A.R. (2003). RNA-modifying enzymes. Curr. Opin. Struct. Biol. *13*, 49–55.

Giegé, R., Sissler, M., and Florentz, C. (1998). Universal rules and idiosyncratic features in tRNA identity. Nucleic Acids Res. *26*, 5017–5035.

Green, R., and Noller, H.F. (1999). Reconstitution of functional 50S ribosomes from in vitro transcripts of *Bacillus stearothermophilus* 23S rRNA. Biochemistry *38*, 1772–1779.

Gregson, J.M., Crain, P.F., Edmonds, C.G., Gupta, R., Hashizume, T., Phillipson, D.W., and McCloskey, J.A. (1993). Structure of the archaeal transfer RNA nucleoside G*-15 (2-amino-4,7-dihydro-4-oxo-7-β-D-ribofuranosyl-1H-pyrrolo[2,3-d]pyrimidine-5-carboximidamide (archaeosine)). J. Biol. Chem. *268*, 10076–10086.

Gupta, R. (1984). *Halobacterium volcanii* tRNAs. Identification of 41 tRNAs covering all amino acids, and the sequences of 33 class I tRNAs. J. Biol. Chem. *259*, 9461–9471.

Gutgsell, N., Englund, N., Niu, L., Kaya, Y., Lane, B.G., and Ofengand, J. (2000). Deletion of the *Escherichia coli* pseudouridine synthase gene truB blocks formation of pseudouridine 55 in tRNA *in vivo*, does not affect exponential growth, but confers a strong selective disadvantage in competition with wild-type cells. RNA *6*, 1870–1881.

Gutgsell, N.S., Del Campo, M.D., Raychaudhuri, S., and Ofengand, J. (2001). A second function for pseudouridine synthases: A point mutant of RluD unable to form pseudouridines 1911, 1915, and 1917 in *Escherichia coli* 23S ribosomal RNA restores normal growth to an RluD-minus strain. RNA *7*, 990–998.

Heiss, N.S., Knight, S.W., Vulliamy, T.J., Klauck, S.M., Wiemann, S., Mason, P.J., Poustka, A., and Dokal, I. (1998). X-linked dyskeratosis congenita is caused by mutations in a highly conserved gene with putative nucleolar functions. Nat. Genet. *19*, 32–38.

Helm, M., Florentz, C., Chomyn, A., and Attardi, G. (1999). Search for differences in post-transcriptional modification patterns of mitochondrial DNA-encoded wild-type and mutant human $tRNA^{Lys}$ and $tRNA^{Leu}_{(UUR)}$. Nucleic Acids Res. *27*, 756–763.

Hoang, C., and Ferré-D'Amaré, A.R. (2001). Cocrystal structure of a tRNA Ψ55 pseudouridine synthase: nucleotide flipping by an RNA-modifying enzyme. Cell *107*, 929–939.

Horie, N., Hara-Yokoyama, M., Yokoyama, S., Watanabe, K., Kuchino, Y., Nishimura, S., and Miyazawa, T. (1985). Two $tRNA^{Ile}1$ species from an extreme thermophile, *Thermus thermophilus* HB8: effect of 2-thiolation of ribothymidine on the thermostability of tRNA. Biochemistry *24*, 5711–5715.

Ishitani, R., Nureki, O., Kijimoto, T., Watanabe, M., Kondo, H., Nameki, N., Okada, N., Nishimura, S., and Yokoyama, S. (2001). Crystallization and preliminary X-ray analysis of the archaeosine tRNA- guanine transglycosylase from *Pyrococcus horikoshii*. Acta Crystallogr. *D57*, 1659–1662.

Ishitani, R., Nureki, O., Fukai, S., Kijimoto, T., Nameki, N., Watanabe, M., Kondo, H., Sekine, M., Okada, N., Nishimura, S., and Yokoyama, S. (2002). Crystal structure of archaeosine tRNA-guanine transglycosylase. J. Mol. Biol. *318*, 665–677.

Jones, T.A., Zou, J.-Y., Cowan, S.W., and Kjeldgaard, M. (1991). Improved methods for binding protein models in electron density maps and the location of errors in these models. Acta Crystallogr. *A47*, 110–119.

Kawai, G., Yamamoto, Y., Kamimura, T., Masegi, T., Sekine, M., Hata, T., Iimori, T., Watanabe, T., Miyazawa, T., and Yokoyama, S. (1992). Conformational rigidity of specific pyrimidine residues in tRNA arises from posttranscriptional modifications that enhance steric interaction between the base and the 2′-hydroxyl group. Biochemistry *31*, 1040–1046.

Khaitovich, P., Tenson, T., Kloss, P., and Mankin, A.S. (1999). Reconstitution of functionally active *Thermus aquaticus* large ribosomal subunits with *in vitro*-transcribed rRNA. Biochemistry *38*, 1780–1788.

Kim, S.H., Quigley, G.J., Suddath, F.L., McPherson, A., Sneden, D., Kim, J.J., Weinzierl, J., and Rich, A. (1973). Three-dimensional structure of yeast phenylalanine transfer RNA: folding of the polynucleotide chain. Science *179*, 285–288.

Kiss, T. (2001). Small nucleolar RNA-guided post-transcriptional modification of cellular RNAs. EMBO J. *20*, 3617–3622.

Kiss, T. (2002). Small nucleolar RNAs: an abundant group of noncoding RNAs with diverse cellular functions. Cell *109*, 145–148.

Lafontaine, D.L., Bousquet-Antonelli, C., Henry, Y., Caizergues-Ferrer, M., and Tollervey, D. (1998). The box H + ACA snoRNAs carry Cbf5p, the putative rRNA pseudouridine synthase. Genes Dev. *12*, 527–537.

Laskowski, R.A., MacArthur, M.W., Morris, A.L., and Thornton, J.M. (1993). PROCHECK: a program to check the stereochemical quality of protein structures. J. Appl. Crystallogr. *26*, 283–291.

Limbach, P.A., Crain, P.F., and McCloskey, J.A. (1994). Summary: the modified nucleosides of RNA. Nucleic Acids Res. *22*, 2183–2196.

Marck, C., and Grosjean, H. (2002). tRNomics: analysis of tRNA genes from 50 genomes of Eukarya, Archaea, and Bacteria reveals anticodon-sparing strategies and domain-specific features. RNA *8*, 1189–1232.

McCloskey, J.A., and Crain, P.F. (1998). The RNA modification database—1998. Nucleic Acids Res. *26*, 196–197.

McCloskey, J.A., Graham, D.E., Zhou, S., Crain, P.F., Ibba, M., Konisky, J., Söll, D., and Olsen, G.J. (2001). Post-transcriptional modification in archaeal tRNAs: identities and phylogenetic relations of nucleotides from mesophilic and hyperthermophilic *Methanococcales*. Nucleic Acids Res. *29*, 4699–4706.

Nicholls, A., Sharp, K.A., and Honig, B. (1991). Protein folding and association: insights from the interfacial and thermodynamic properties of hydrocarbons. Proteins *11*, 281–296.

Ofengand, J. (2002). Ribosomal RNA pseudouridines and pseudouridine synthases. FEBS Lett. *514*, 17–25.

Ohtsuki, T., Kawai, G., and Watanabe, K. (2002). The minimal tRNA: unique structure of *Ascaris suum* mitochondrial $tRNA^{Ser}_{(UCU)}$ having a short T arm and lacking the entire D arm. FEBS Lett. *514*, 37–43.

Okimoto, R., and Wolstenholme, D.R. (1990). A set of tRNAs that lack either the T ψ C arm or the dihydrouridine arm: towards a minimal tRNA adaptor. EMBO J. *9*, 3405–3411.

Okimoto, R., Macfarlane, J.L., Clary, D.O., and Wolstenholme, D.R. (1992). The mitochondrial genomes of two nematodes, *Caenorhabditis elegans* and *Ascaris suum*. Genetics *130*, 471–498.

Otwinowski, Z., and Minor, W. (1997). Processing of X-ray diffraction data collected in oscillation mode. In Methods in Enzymology, J. Carter, C.W., and R. M. Sweet, eds. (Academic Press), pp. 307–326.

Roe, B.A., Ma, D.P., Wilson, R.K., and Wong, J.F. (1985). The complete nucleotide sequence of the *Xenopus laevis* mitochondrial genome. J. Biol. Chem. *260*, 9759–9774.

Sanner, M.F., Olson, A.J., and Spehner, J.-C. (1995). Fast and robust computation of molecular surfaces. Proc. 11th ACM Symp. Comp. Geom., 104–106.

Shi, H., and Moore, P.B. (2000). The crystal structure of yeast phenylalanine tRNA at 1.93 Å resolution: a classic structure revisited. RNA *6*, 1091–1105.

Sprinzl, M., Horn, C., Brown, M., Ioudovitch, A., and Steinberg, S. (1998). Compilation of tRNA sequences and sequences of tRNA genes. Nucleic Acids Res. *26*, 148–153.

Vagin, A., and Teplyakov, A. (1997). MOLREP: an automated program for molecular replacement. J. Appl. Crystallogr. *30*, 1022–1025.

Watanabe, M., Matsuo, M., Tanaka, S., Akimoto, H., Asahi, S., Nishimura, S., Katze, J.R., Hashizume, T., Crain, P.F., McCloskey, J.A., and Okada, N. (1997). Biosynthesis of archaeosine, a novel derivative of 7-deazaguanosine specific to archaeal tRNA, proceeds via a pathway involving base replacement on the tRNA polynucleotide chain. J. Biol. Chem. *272*, 20146–20151.

Watanabe, M., Nameki, N., Matsuo-Takasaki, M., Nishimura, S., and

Okada, N. (2000). tRNA recognition of tRNA-guanine transglycosylase from a hyperthermophilic archaeon, *Pyrococcus horikoshii*. J. Biol. Chem. *276*, 2387–2394.

Watkins, N.J., Gottschalk, A., Neubauer, G., Kastner, B., Fabrizio, P., Mann, M., and Luhrmann, R. (1998). Cbf5p, a potential pseudouridine synthase, and Nhp2p, a putative RNA-binding protein, are present together with Gar1p in all H BOX/ACA-motif snoRNPs and constitute a common bipartite structure. RNA *4*, 1549–1568.

Wolstenholme, D.R., Macfarlane, J.L., Okimoto, R., Clary, D.O., and Wahleithner, J.A. (1987). Bizarre tRNAs inferred from DNA sequences of mitochondrial genomes of nematode worms. Proc. Natl. Acad. Sci. USA *84*, 1324–1328.

Yokoyama, S., and Nishimura, S. (1995). Modified nucleosides and codon recognition. In tRNA: Structure, Biosynthesis, and Function, D. Söll, and U. RajBhandary, eds. (ASM Press), pp. 207–223.

Accession Numbers

The coordinates and the structure factors have been deposited in the PDB with the accession code 1J2B.